Datasheet for 600-401-103-0.1

Collagen Type I Antibody

Overview

Description:	Anti-Collagen Type I (RABBIT) Antibody - 600-401-103-0.1
Item No.:	600-401-103-0.1
Size:	100 µg
Applications:	Dot Blot, IHC, WB, ELISA, EM, FC, IF, IP, Multiplex
Reactivity:	Human, Mouse, Rat, Bovine, Pig
Host Species:	Rabbit

Product Details

Background:	Rockland produces highly active antibodies and conjugates to collagens. Collagens are highly conserved throughout evolution and are characterized by an uninterrupted ''Glycine-X-Y'' triplet repeat that is a necessary part of the triple helical structure. For these reasons, it is often extremely difficult to generate antibodies with specificities to collagens. The development of 'type' specific antibodies is dependent on NON-DENATURED three-dimensional epitopes. Rockland extensively purifies collagens for immunization from human and bovine placenta and cartilage by limited pepsin digestion and selective salt precipitation. This preparation results in a native conformation of the protein. Antibodies are isolated from rabbit antiserum and are extensively cross-adsorbed by immunoaffinity purification to produce 'type' specific antibodies. Greatly diminished reactivity and selectivity of these antibodies will result if denaturing and reducing conditions are used for SDS-PAGE and immunoblotting. Ideal for investigators involved in Cell Biology, Signal Transduction and Stem Cell research.
Synonyms:	rabbit anti-collagen type I antibody, Collagen Of Skin Tendon And Bone, Collagen Type 1 antibody, Collagen type I alpha 1 antibody, Collagen alpha-1 (I) chain, Alpha-1 type I collagen, type 1 procollagen alpha 1
Host Species:	Rabbit
Clonality:	Polyclonal
Format:	IgG

Target Details

Gene Name:	COL1A1/A2

Reactivity:	Human, Mouse, Rat, Bovine, Pig
Immunogen Type:	Native Protein
Immunogen:	Collagen Type I from human and bovine placenta
Purity/Specificity:	COLLAGEN I Antibody has been prepared by immunoaffinity chromatography using immobilized antigens. Some class-specific anti-collagens may be specific for three-dimensional epitopes which may result in diminished reactivity with denatured collagen or formalin-fixed, paraffin embedded tissues. This antibody reacts with most mammalian Type I collagens and has expected cross-reactivity with Type III and negligible cross reactivity with Type II, IV, V or VI collagens. Non-specific cross-reaction of anti-collagen antibodies with other human serum proteins or non-collagen extracellular matrix proteins has not been tested.
Relevant Links:	• 600-401-103 SDS • Anti-Collagen IHC Protocol • UniProtKB - P08123 • UniProtKB - P02452 • NCBI - NP_000079.2 • GeneID - 1277

Application Details

Tested Applications:	Dot Blot, IHC, WB
Suggested Applications:	ELISA, EM, FC, IF, IP, Multiplex (Based on references)
Application Note:	Anti-Collagen Type I has been tested by Western blot, dot blot, and IHC and is suitable for indirect trapping ELISA for quantitation of antigen in serum using a standard curve, IP, native PAGE, immunofluorescence, and FC for highly sensitive qualitative analysis.
Assay Dilutions:	All assays should be optimized by the user. Recommended dilutions (if any) may be listed below.
ELISA:	1:5,000 - 1:50,000
FC:	User Optimized
FLISA:	1:100
IF:	User Optimized
IHC:	1:50 - 1:200
IP:	1:100
WB:	1:1,000 - 1:10,000

Formulation

Physical State:	Liquid (sterile filtered)
Concentration:	1.09 mg/mL by UV absorbance at 280 nm
Buffer:	0.02 M Potassium Phosphate, 0.15 M Sodium Chloride, pH 7.2
Preservative:	0.01% (w/v) Sodium Azide
Stabilizer:	None

Shipping & Handling

Shipping Condition:	Wet Ice
Storage Condition:	Store vial at 4° C prior to opening. This product is stable at 4° C as an undiluted liquid. Dilute only prior to immediate use. For extended storage, mix with an equal volume of glycerol, aliquot contents and freeze at -20° C or below. Avoid cycles of freezing and thawing.
Expiration:	Expiration date is one (1) year from date of receipt.

Images

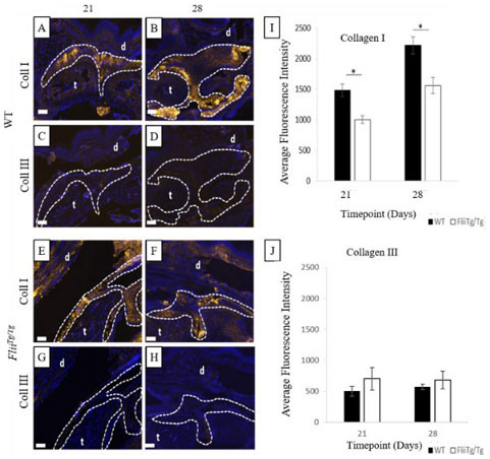

Immunohistochemistry
Immunohistochemistry of Anti-Collagen Type I.
WT mice have significantly increased collagen type I expression in the tendon adhesions. Representative images of collagen type I expression (gold) in the tendon adhesions of WT (a-b) and FliiTg/Tg (e-f) mice and collagen type III expression (gold) in the tendon adhesions of WT (c-d) FliiTg/Tg (g-h) at 21 and 28 days post 50% partial laceration injury. (i) WT mice have significantly upregulated collagen type I levels in the adhesions compared with FliiTg/Tg mice. (j) No significant difference was noted in collagen type III levels in WT and FliiTg/Tg mice, although detectable levels of collagen type III were found in the FliiTg/Tg mice. DAPI is represented as blue fluorescence; t, tendon; d, dermis. Dotted line represents tendon adhesion area. Magnification × 10. Scale bar = 200 µM and refers to all images. Data represented as mean ± SEM. *p ≤ 0.05. n = 6.
Fig 7. PMID: 32854733.

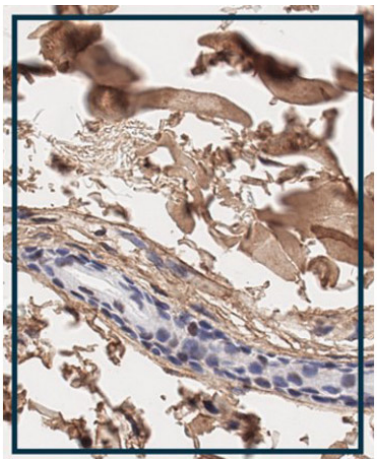

Immunohistochemistry
Immunohistochemistry using Rabbit Anti-Collagen Type I Antibody.
Tissue: Human Skin.
Fixation: formalin fixed paraffin embedded.
Antigen retrieval: HEIR pH 6.0 buffer for 20 mins.
Primary antibody: Anti-Collagen Type I Antibody (lot 52110) at 1:500 for 30 mins.
Secondary antibody: Anti-Rabbit Poly-HRP IgG for 8 mins.
Staining: DAB kit. Localization: Peri-follicular and dermal collagen.
Size: W 164.6µm x L 206.2µm.

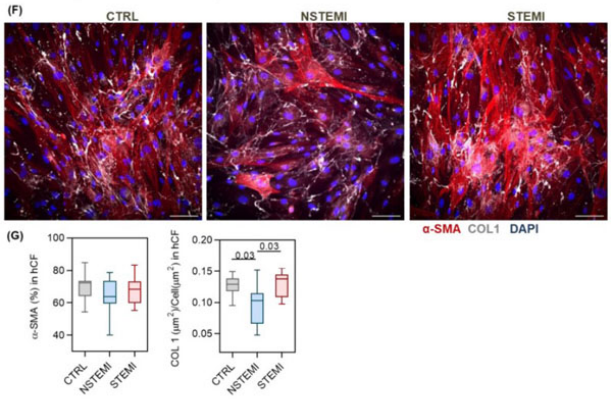

Immunofluorescence Microscopy
Immunofluorescence results using Rabbit Anti-Collagen Type I Antibody. hCFs were fixed with 4% paraformaldehyde, and then cells were permeabilized with 0.1% Triton X-100 for 5 min. Samples were blocked with 1% BSA + 4% FBS and incubated with the primary antibodies α-smooth muscle actin (SMA) and collagen type I (p/n 600-401-103) and respective secondary antibodies. Cell nuclei were stained with 4',6'-diamino-2-fenil-indol (DAPI; 5 µg/mL). (F,G) Representative images and respective quantification of the alpha-smooth muscle actin (α-SMA) and collagen type I (α-COL I) of hCFs cultured in 2% pericardial fluid. Pericardial fluid is a reservoir of fibrosis-related molecules and induces cardiac fibroblast activation. Fig 2. PMID: 39125899.

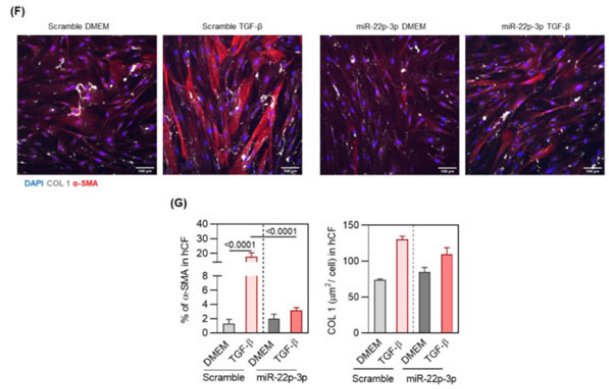

Immunofluorescence Microscopy
Immunofluorescence results using Rabbit Anti-Collagen Type I antibody. hCFs were fixed with 4% paraformaldehyde, and then cells were permeabilized with 0.1% Triton X-100 for 5 min. Samples were blocked with 1% BSA + 4% FBS and incubated with the primary antibodies α-smooth muscle actin (SMA) and collagen type I (p/n 600-401-103) and respective secondary antibodies. Cell nuclei were stained with 4',6'-diamino-2-fenil-indol (DAPI; 5 µg/mL). miR-22-3p overexpression inhibits hCF activation in vitro. (F) Representative figures of α-SMA and COL I in transfected hCFs following a 7-day activation assay. (G) Percentage of α-SMA + cells (n = 4/group) and area of COL I per cell (n = 2/group). Fig 4. PMID: 39125899.

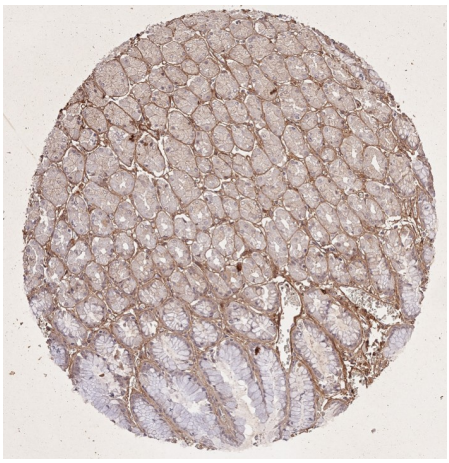

Immunohistochemistry
Immunohistochemistry results of Rabbit Anti-Collagen Type I Antibody.
Tissue: human stomach mucosa (TMA).
Fixation: FFPE.
Antigen Retrieval: HIER using Tris-EDTA-citrate buffer pH 7.8 for 5 min.
Blocking: Peroxidase-Blocking Solution for 10 min.
Primary Antibody: Anti-Collagen Type I (p/n 600-401-103-0.1) at 1:15 for 1 hr at 37 °C.
Secondary Antibody: Dako REAL EnVision Detection Kit, Polymer-HRP, Rabbit/Mouse.
Counterstain: Hematoxylin for 15 sec.
Substrate: DAB-Chromogen, Rabbit/Mouse.
Staining/Results: basement membranes and blood vessels.
Independently Validated by antibodies-online GmbH (p/n ABIN7565871/ ABIN5596819/ ABIN5596820) by MS Validated Antibodies.

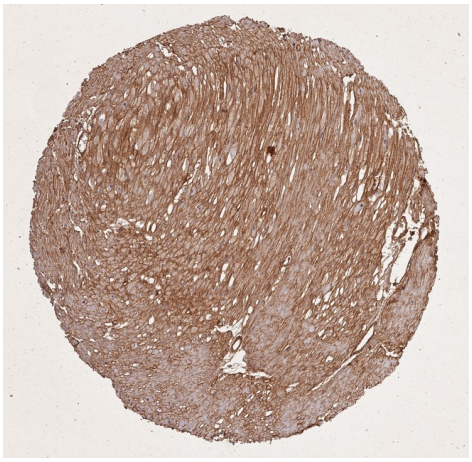

Immunohistochemistry
Immunohistochemistry results of Rabbit Anti-Collagen Type I Antibody.
Tissue: smooth muscle cells of human stomach wall.
Fixation: FFPE.
Antigen Retrieval: HIER using Tris-EDTA-citrate buffer pH 7.8 for 5 min.
Blocking: Peroxidase-Blocking Solution for 10 min.
Primary Antibody: Anti-Collagen Type I (p/n 600-401-103-0.1) at 1:15 for 1 hr at 37 °C.
Secondary Antibody: Dako REAL EnVision Detection Kit, Polymer-HRP, Rabbit/Mouse.
Counterstain: Hematoxylin for 15 sec.
Substrate: DAB-Chromogen, Rabbit/Mouse.
Staining/Results: smooth muscle cells surrounded by collagen fibers.
Independently Validated by antibodies-online GmbH (p/n ABIN7565871/ ABIN5596819/ ABIN5596820) by MS Validated Antibodies.

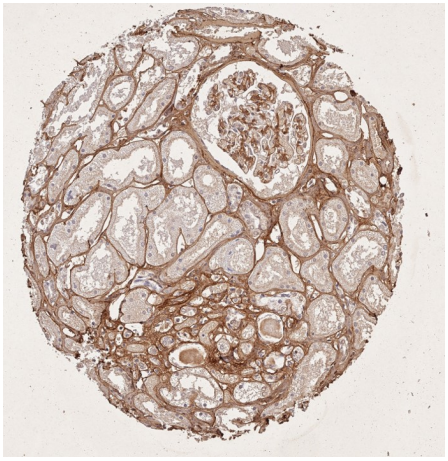

Immunohistochemistry
Immunohistochemistry results of Rabbit Anti-Collagen Type I Antibody.
Tissue: human tubuli and blood vessels.
Fixation: FFPE.
Antigen Retrieval: HIER using Tris-EDTA-citrate buffer pH 7.8 for 5 min.
Blocking: Peroxidase-Blocking Solution for 10 min.
Primary Antibody: Anti-Collagen Type I (p/n 600-401-103-0.1) at 1:15 for 1 hr at 37 °C.
Secondary Antibody: Dako REAL EnVision Detection Kit, Polymer-HRP, Rabbit/Mouse.
Counterstain: Hematoxylin for 15 sec.
Substrate: DAB-Chromogen, Rabbit/Mouse.
Staining/Results: Intense collagen I staining of fibres surrounding tubuli and around blood vessels.
Independently Validated by antibodies-online GmbH (p/n ABIN7565871/ ABIN5596819/ ABIN5596820) by MS Validated Antibodies.

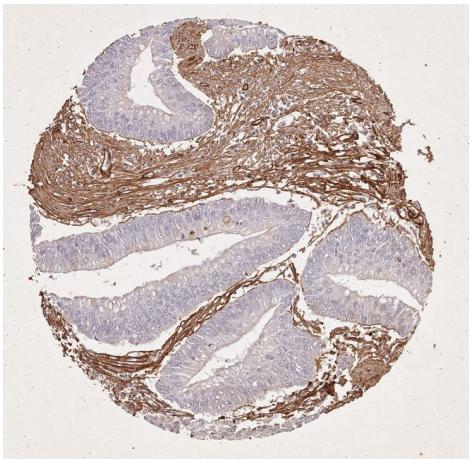

Immunohistochemistry
Immunohistochemistry results of Rabbit Anti-Collagen Type I Antibody.
Tissue: human stroma of a colorectal adenocarcinoma.
Fixation: FFPE.
Antigen Retrieval: HIER using Tris-EDTA-citrate buffer pH 7.8 for 5 min.
Blocking: Peroxidase-Blocking Solution for 10 min.
Primary Antibody: Anti-Collagen Type I (p/n 600-401-103-0.1) at 1:15 for 1 hr at 37 °C.
Secondary Antibody: Dako REAL EnVision Detection Kit, Polymer-HRP, Rabbit/Mouse.
Counterstain: Hematoxylin for 15 sec.
Substrate: DAB-Chromogen, Rabbit/Mouse.
Staining/Results: Cancer cells are collagen I negative.
Independently Validated by antibodies-online GmbH (p/n ABIN7565871/ ABIN5596819/ ABIN5596820) by MS Validated Antibodies.

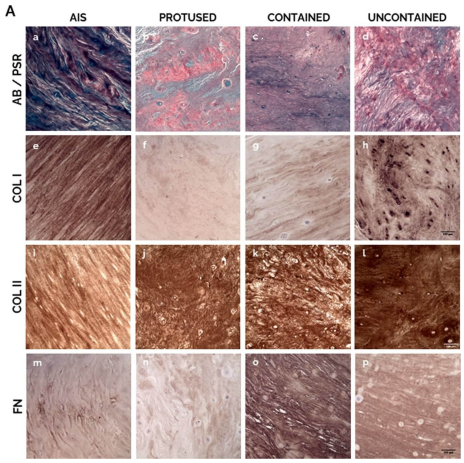

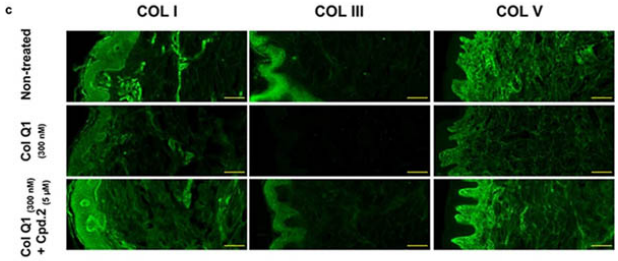

Immunohistochemistry

Human AF matrix biochemical characterization with herniation progression. A) Histological/IHC staining for a–d: Alcian Blue/Picro-Sirius Red, scale bar: 100 µm; e–h: Collagen I, scale bar: 100 µm; i–l: Collagen II, scale bar: 100 µm; m–p: Fibronectin, scale bar: 100 µm. B) Quantification of each staining per herniation type. Data presented using dot plots, with median and interquartile range. Kruskal-Wallis test followed by corrected Dunn's were performed. *p < 0.05; **p < 0.01. C) Multivariate analysis of interaction of hernia containment level with age for each staining Figure provided by CiteAb. Source: Arthritis Res Ther, PMID: 35039075.

Immunocytochemistry

Compound 2 suppressed the collagenolytic effect of ColQ1 ex vivo in pig skin tissue. a) Dose-dependent effect of compound 2 quantified by Hyp release assay. b) Confocal SHG images showed an improved COL signal with 5 √ó 10,àí6 m of compound 2 (tissue challenged with 300 √ó 10,àí9 M ColQ1) compared with 300 √ó 10,àí9 M ColQ1 without inhibitor. c) Immunostaining of fibrillar COLs of the non-treated pig skin and treated with ColQ1 with or without compound 2. Statistical analysis was performed with one-way ANOVA and statistical significance was analyzed by Tukey test. Significance was calculated by comparing non-treated versus treated tissue with compound 2 (mean ¬± SD, *** p ‚â§ 0.001, ** p ‚â§ 0.01). Hyp: hydroxyproline, COL: collagen, SHG: second harmonic generation. Scale bar: 100 Œºm for SHG images and 100 Œºm for the immunostained images. Figure provided by CiteAb. Source: Adv Ther (Weinh), PMID: 35310821.

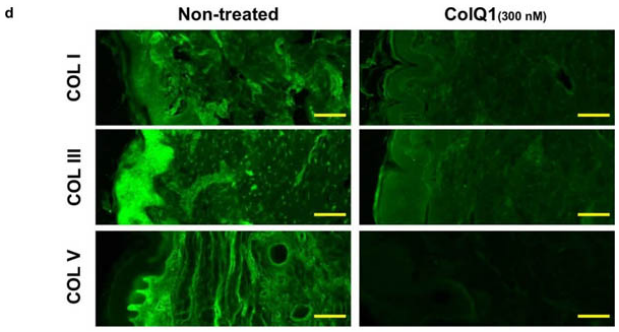

Immunocytochemistry

The effect of ColQ1 on dermal COL of pig-skin. a,b) Quantification of Hyp release over time after treatment with different concentrations of a) B. cereus csn (0,àí100% v/v) and b) ColQ1 (0,àí500 √ó 10,àí9 M). This graph contains data adapted from our previous publication. [38] c) Confocal SHG Z-stack images of the COL structure in skin dermal region that was non-treated or treated with 300 √ó 10,àí9 M ColQ1. d) B. cereus ColQ1 (300 √ó 10,àí9 M) degraded the fibrillar COLs, immunostaining of non-treated and ColQ1 treated pig skin with COL antibodies (COL I, III, and V). COL: collagen, Hyp: hydroxyproline, B. cereus: Bacillus cereus, csn: culture supernatant, SHG: second harmonic generation. Data point represents mean value ¬± standard deviation (n = 3). Scale bar: 100 Œºm for SHG images and immunostained images. Bright-field and DAPI images of the immunostained non-treated and ColQ1-treated tissue are shown in Figure S4, Supporting Information. Figure provided by CiteAb. Source: Adv Ther (Weinh), PMID: 35310821.

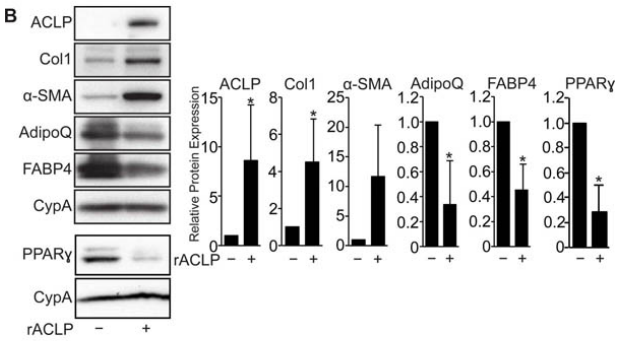

Western Blot

ACLP signaling represses adipogenesis. A, Scheme of 10T1/2 adipogenesis and rACLP treatment. B, 10T1/2 fibroblasts were treated with 30 nM rACLP on days -2, -1, 0, +2 and +4 and induced to undergo adipogenesis with DMII on day 0. Protein was harvested on day +6 and analyzed by SDS-PAGE and Western blot with antibodies against ACLP, collagen, Œ±-SMA, AdipoQ, FABP4, PPARŒ≥ and cyclophilin-a (CypA). PPARŒ≥ analysis was performed in separate experiments. Protein expression was quantified by densitometry normalized to CypA expression and relatively compared to control cells. *, p < 0.05 versus control, one sample t-test for all values. C, 10T1/2 fibroblasts were treated with 30 nM rACLP on days -2, -1, 0, +2 and +4 and induced to undergo adipogenesis with DMII on day 0. On day +6 cells were fixed, stained, imaged and quantified with Oil Red O dye (n = 3). Data were normalized relative to untreated controls. *, p < 0.05 versus paired control, one sample t-test. Data presented are expressed as mean ¬± SD. The scale bar represents 2 mm. Figure provided by CiteAb. Source: PLoS One, PMID: 29799877.

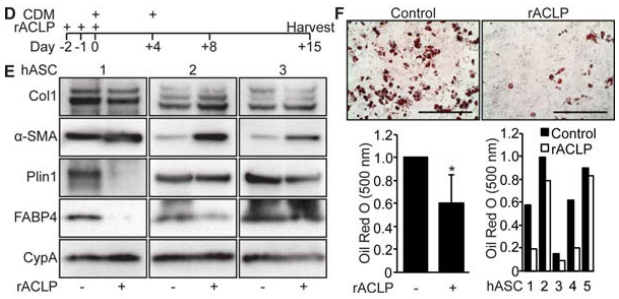

Western Blot

Recombinant ACLP inhibits adipogenesis and enhances myofibroblast differentiation in human adipose stromal cells. A, Scheme of time course for adipogenesis of hASC. B, hASC derived from subcutaneous adipose depots were induced to undergo adipogenesis with CDM on day 0. Protein was harvested on days 0, +1, +2, +8 and +15. Protein expression was analyzed using SDS-PAGE and Western blot with antibodies against ACLP, Œ±-SMA, FABP4 and cyclophilin-A. C, Omental hASC were induced to undergo adipogenesis with CDM on day 0. Protein was harvested on days 0, +1, +2, +8 and +15. Protein expression was analyzed using SDS-PAGE and Western blot with antibodies against ACLP, Œ±-SMA, FABP4 and cyclophilin-A. D, Scheme of adipogenesis for hASC and rACLP treatment. E, Subcutaneous hASC were treated with 30 nM rACLP on days -2, -1 and 0 and induced to undergo adipogenesis with CDM on day 0 and +4. Protein was harvested on day +15 and analyzed by SDS-PAGE and Western blot with antibodies against collagen, Œ±-SMA, perilipin, FABP4 and CypA (n = 3). F, Subcutaneous hASC were treated with 30 nM rACLP on days -2, -1, and 0 and induced to undergo adipogenesis with CDM on day 0 and +4. On day +15 cells were fixed, stained, imaged and quantified with Oil Red O dye (n = 5). Data were normalized relative to control. * p < 0.05 versus control. Data presented are expressed as mean ¬± SD. The scale bar represents 2 mm. Figure provided by CiteAb. Source: PLoS One, PMID: 29799877.

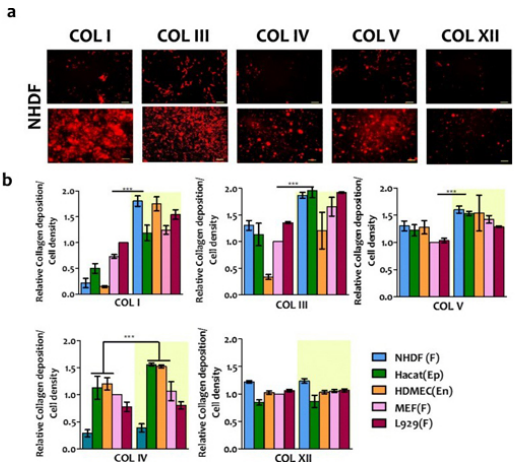

Immunofluorescence Microscopy

Quantification of H47 stimulated deposition of different collagen subtypes. a. Fluorescence images showing immunostained COL I, III, IV, V and XII in NHDF cells before and after treatment with 0.5 µM H47 (Scale – 250 µm) b. Quantification of deposited COL I, III, IV, V and XII from immuno-stained images in NHDF, L929, MEF, HaCaT and HDMEC cultures. Data correspond to collagen deposition 24 h after H47 treatment and controls. The plots were normalized with MEF cells untreated condition as 1. Error bars represent standard deviation from n-3 experiments. Statistical significance was analyzed by Tukey test comparing non treated against H47 treated cells (mean ± SD, ANOVA, *** p < 0.001). Fig 4. PMID: 32228452

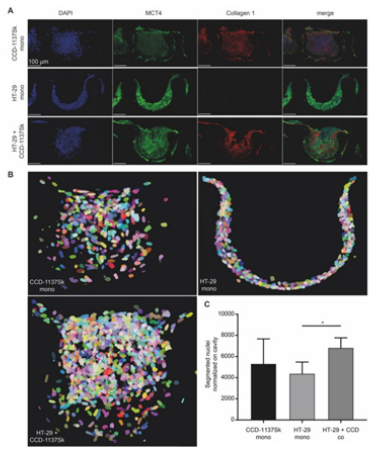

Immunofluorescence Microscopy
Chip-based 3-D cultures reveal morphological and metabolic changes upon co-cultivation of HT-29 and CCD-1137Sk cells. A total of 4000 cells per chip cavity were seeded to yield either mono- or co-cultures of HT-29 and CCD-1137Sk cells. In the case of co-cultures, 2000 HT-29 cells were co-seeded with 2000 CCD-1137Sk cells per well. After four days, chips were fixed, transversally sectioned, and then stained with DAPI as well as antibodies against MCT4 and collagen 1 as markers for nuclei, lactate export, and extracellular matrix (ECM), respectively. Subsequently, sections were imaged with confocal microscopy. (A) Representative maximum-z projections. (B) Representative display of segmented nuclei from different culture conditions as indicated. Pseudo-colors were chosen to discriminate between individual nuclei. They do not indicate different cell types. (C) Quantitative analysis of nuclear counts. Mean + SEM (n = 3 experiments). Fig 5. PMID: 32823793

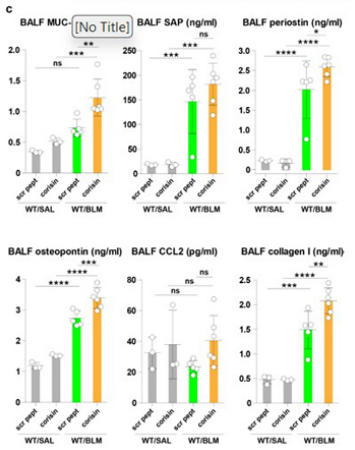

ELISA
c) The BALF levels of serum amyloid P component (SAP), MUC-1, chemokine (C-C motif) ligand 2 (CCL2), periostin, collagen I, and osteopontin were measured by enzyme immunoassays following the manufacturer's instructions. The number of mice: n=3 in WT/SAL/scr pept and WT/SAL/corisin groups, n=5 in WT/BLM/scr pept, and n=6 in WT/BLM/corisin group. Data are the mean ± S.D. Statistical analysis by ANOVA with a post hoc Newman-Keuls test. *p<0.05; **p<0.01; ***p<0.001; ****p<0.0001. ns, not significant. SF22. PMID: 35322016

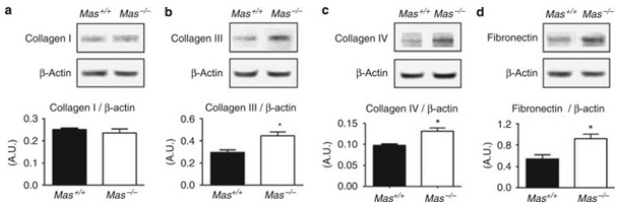

Western Blot
Immunoblotting of extracellular matrix (ECM) proteins in kidneys of Mas+/+ and Mas−/− animals. (a) Immunoblotting shows no difference of Collagen I (p/n 600-401-103) expression in Mas+/+ and Mas−/− mice kidneys. Significant increases in (b) Collagen III (p/n 600-401-105), (c) Collagen IV (p/n 600-401-106), and (d) fibronectin (p/n 600-401-117) expression were detected by comparing immunoblots of Mas−/− mouse kidneys with those of Mas+/+ controls. Each band represents one mouse kidney from either Mas+/+ or Mas−/− mice. Data are shown as the mean±s.e.m. *P<0.05. A.U. indicates arbitrary unit. Fig 5. PMID: 19262461

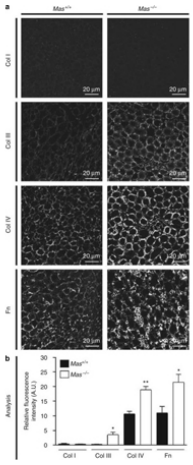

Immunofluorescence Microscopy
Immunofluorescence of extracellular matrix (ECM) proteins in the medulla of kidneys from Mas+/+ (left column) and Mas−/− (right column) mice. (a) Fluorescence (Cy3-labeled anti-rabbit IgG) reveals the immunolabeling of ECM proteins. Expression of type III collagen (Col III) (p/n 600-401-105), type IV collagen (Col IV) (p/n 600-401-106), and fibronectin (Fn) (p/n 600-401-117) were increased in the medulla of Mas−/− compared with that of Mas+/+ mice, whereas the expression of type I collagen (Col I) (p/n 600-401-103) was unaltered. (b) Quantification of ECM proteins in the medulla of Mas+/+ and Mas−/− mice. Data are shown as mean±s.e.m. *P<0.05; **P<0.01. A.U. indicates arbitrary unit. Fig 3. PMID: 19262461

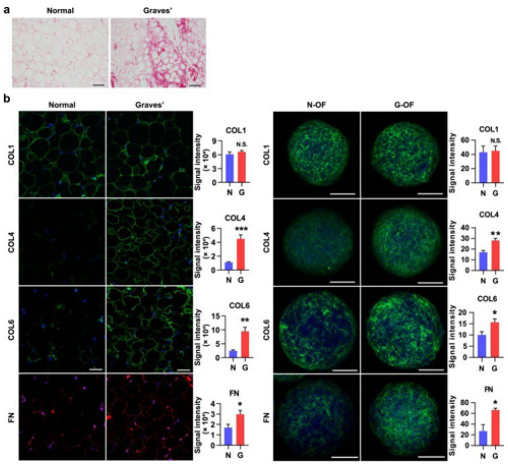

Immunofluorescence Microscopy
Unique ECM deposition in GO tissues and GO-derived OF organoids. (a) Representative Sirius red staining of periocular adipose tissues in control (normal) and GO (Graves). Scale bars, 100 µm. (b) Representative immunofluorescent staining of collagens (green) and FN (red or green) with DAPI (blue) in control and Graves orbital adipose tissues (left, n = 4 to 5) and 3D organoids reconstituted from hOFs isolated from respective tissues (right). Signal intensities were quantified per spheroid. n = 5 to 8 organoids. Scale bars, 50 µm (left) and 100 µm (right). G indicates G-OF; N indicates N-OF. *P < 0.05, unpaired Student t test (n = 4 in each group). Fig 2. PMID: 30388216

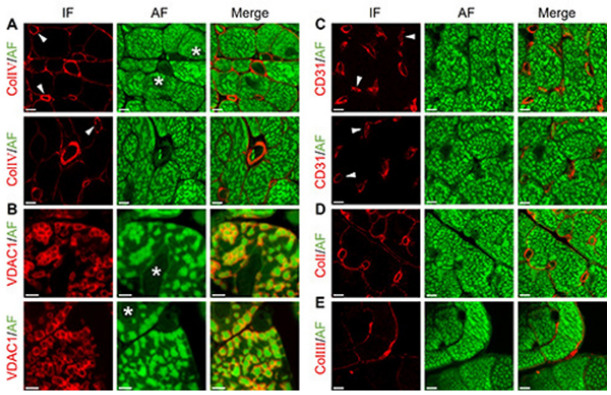

Immunofluorescence Microscopy
Major autofluorescent structures in formaldehyde-fixed mouse myocardial samples identified by IF stainings of (A) Col IV, (B) VDAC1, (C) CD31, (D) Col I (p/n 600-401-103, and (E) Col III (p/n 600-401-105). Images were acquired at cardiomyocyte cross-sectional areas. IF staining (red) allows the localization of basement membrane (Col IV), mitochondria (VDAC1), microvascular endothelial cells (CD31), and interstitial collagen network (Col I and Col III), facilitating the identification of observable structures in AF images (green) acquired at CH1 (525±25 nm). Oval-to-rectangular nuclei (star signs) are observed within cardiomyocytes, and erythrocytes are present within some capillaries (arrowheads). Scale bars: A,C-E) 5 µm; B) 2 µm. Fig 3.
PMID: 37781779

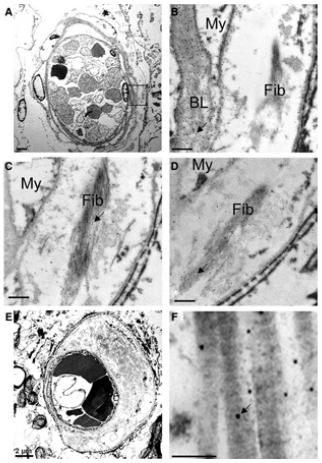

Immunofluorescence Microscopy
Immuno-electron microscopy of collagens I, III, and IV in small vessel disease (SVD). Transmission electron micrographs of small arteries in white matter from older persons with SVD. A–D, Semi-serial sections of a small arteriole, shown at low magnification in A and at higher magnification in B–D with immunogold labeling for collagen-IV (p/n 600-401-106) (B), collagen-I (p/n 600-401-103) (C), or collagen-III (p/n 600-401-105) (D). The region shown at higher magnification in B–D is marked in A (box). Arrows show examples of immunogold particles. In B, collagen-IV labeling shows numerous gold particles over the homogenous basal laminae (BL), behind the endothelium. Mural collagen fibrils (Fib) and myocytes (My) are unlabeled. C, Collagen-I, in contrast to collagen-IV, is mainly localized to the collagen fibrils. D, Collagen-III also labels the banded collagen fibrils. A few gold particles are found over the basal laminae. E and F, Another small artery with severe fibrosis. Low magnification view (E) shows heavy deposits of fibrillar collagens in the vessel wall. In higher magnification, these are heavily labeled for collagen-I (F). Scale bars: 2 µm (A and E), 0.5 µm (B–D), and 0.2 µm (F). Fig 3.
PMID: 36205142

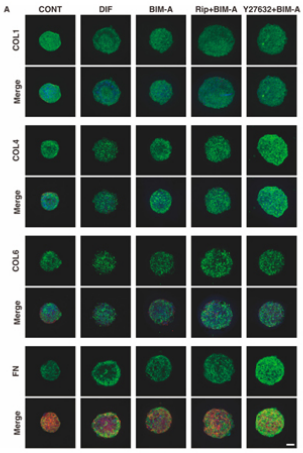

Immunofluorescence Microscopy
Representative confocal images showing the expression of ECMs in 3D 3T3-L1 spheroids under several sets of conditions. (A) On Day 7, the 3D cultures of spheroids of 3T3-L1 preadipocytes as the control (CONT), and their adipogenic differentiation in the absence (DIF) or presence of 100 nM bimatoprost free acid (BIM-A) and/or 10 μM ROCK-i (Rip or Y27632), were immunostained with specific antibodies of ECMs designated by the green color. Scale bar: 100 μm. Fig 9.
PMID: 36421103

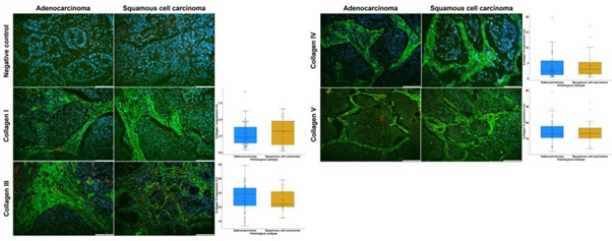

Immunofluorescence Microscopy
Immunofluorescence expression of collagens in the extracellular matrix in lung adenocarcinoma and lung squamous cell carcinoma. The panel shows the negative control, collagen I, collagen III, collagen IV and collagen V. Also as presented the respectively box-plots show the differences of expression between the histological subtypes. The red square in the graphs represents the average expression of the marker for each of the groups. Magnification: 400×. Scale: 100 μm. Fig. 2. PMID: 39938232

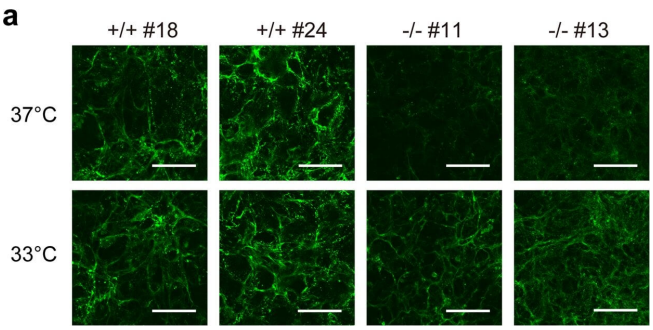

Immunocytochemistry
Immunofluorescence staining of extracellular and intracellular type I collagen. (a) Immunofluorescence staining of type I collagen secreted from MEF clones was performed with an anti-type I collagen antibody without cell permeabilization. Scale bars: 100 μm. (b,c) Immunofluorescence staining of permeabilized MEF clones was performed with anti-type I collagen (green) and anti-KDEL antibodies (red) (b) or anti-type I collagen (green) and anti-GM130 antibodies (red). (c) Scale bars: 10 μm. Figure provided by CiteAb. Source: Sci Rep, PMID: 31758055.

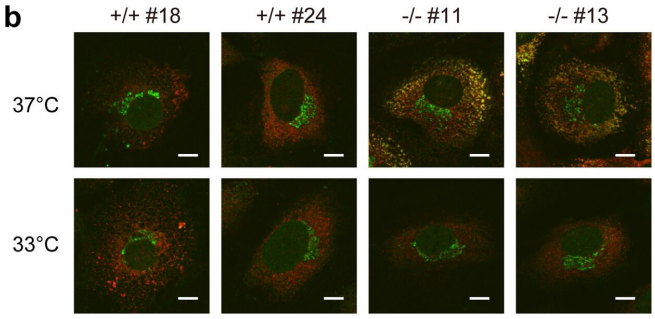

Immunocytochemistry
Immunofluorescence staining of extracellular and intracellular type I collagen. (a) Immunofluorescence staining of type I collagen secreted from MEF clones was performed with an anti-type I collagen antibody without cell permeabilization. Scale bars: 100 µm. (b,c) Immunofluorescence staining of permeabilized MEF clones was performed with anti-type I collagen (green) and anti-KDEL antibodies (red) (b) or anti-type I collagen (green) and anti-GM130 antibodies (red). (c) Scale bars: 10 µm. Figure provided by CiteAb. Source: Sci Rep, PMID: 31758055.

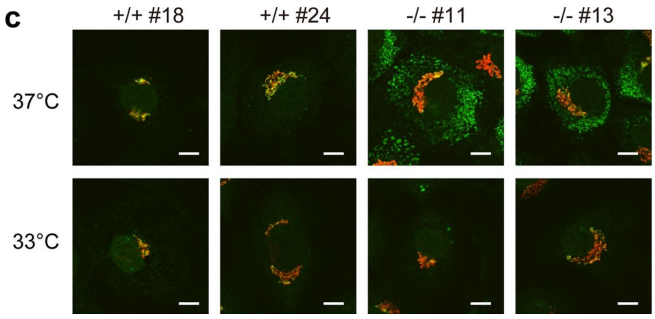

Immunocytochemistry
Immunofluorescence staining of extracellular and intracellular type I collagen. (a) Immunofluorescence staining of type I collagen secreted from MEF clones was performed with an anti-type I collagen antibody without cell permeabilization. Scale bars: 100 µm. (b,c) Immunofluorescence staining of permeabilized MEF clones was performed with anti-type I collagen (green) and anti-KDEL antibodies (red) (b) or anti-type I collagen (green) and anti-GM130 antibodies (red). (c) Scale bars: 10 µm. Figure provided by CiteAb. Source: Sci Rep, PMID: 31758055.

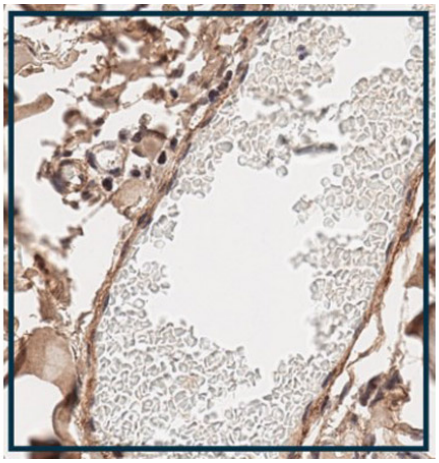

Immunohistochemistry
Immunohistochemistry using Rabbit Anti-Collagen Type I Antibody.
Tissue: Human Skin.
Fixation: formalin fixed paraffin embedded.
Primary antibody: Anti-Collagen Type I Antibody (lot 52110) at 1:500 for 30 mins.
Secondary antibody: Anti-Rabbit Poly-HRP IgG for 8 mins.
Antigen retrieval: HEIR pH 6.0 buffer for 20 mins.
Staining: DAB kit.
Localization: Vessel and dermal Collagen.
Size: W 193.0µm x L 202.7µm.

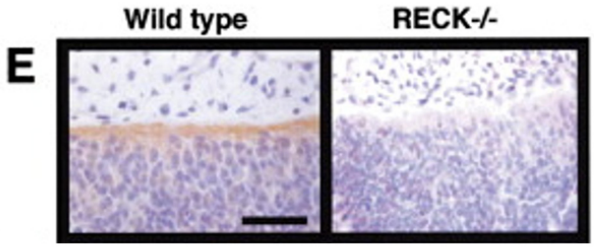

Immunohistochemistry
(E) Effects of the RECK mutation on ECM proteins. The borders between neuroepithelium and mesenchyme in the wild-type (left) or the RECK−/− (right) E10.5 embryo stained with antibodies against collagen I. Fig 3. PMID: 11747814

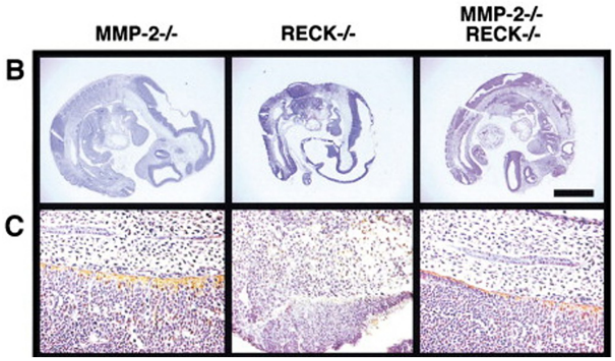

Immunohistochemistry
(B-C) Sections of the E10.5 embryos with genotypes indicated on the top were stained with hematoxylin-eosin (B) or antibodies against collagen I (C). Scale bar: 1 mm in B; 100 µm in C. Fig 5. PMID: 11747814

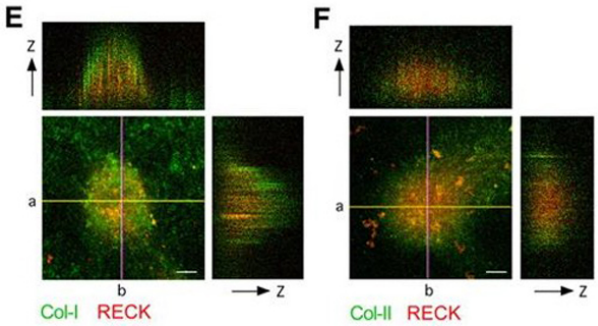

Immunofluorescence Microscopy
(E and F) Localization of type I and type II collagen at cartilaginous nodules formed by ATDC5 cells. ATDC5 cells incubated for 15 days were fixed and stained with anti-RECK (red) plus anti-type I collagen (green; E) or anti-RECK (red) plus anti-type II collagen (green; F). Reconstituted z-axis images along two cutting lines (a,b) are shown in the top and right panels, respectively. Bars, 100 µm in E,F. Fig 2. PMID: 17298979

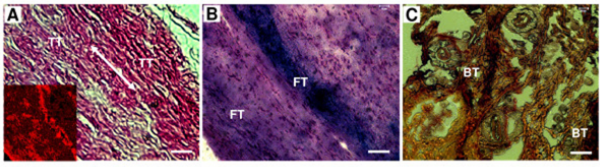

Immunohistochemistry
The testing of multi-differentiation of rabbit TSCs in vivo. A. Formation of tendon-like tissue (TT) revealed by H&E staining and immunohistochemical staining for collagen type I. The collagen fibers are parallel to each other (double arrow), indicative of formation of tendon-like tissue (inset: collagen type I staining). B. Formation of fibrocartilage-like tissue (FT) (Alcian blue staining); and C. formation of bone-like tissue (BT) (Alizarin Red S staining). (Bars: 50 µm). Fig 4. PMID: 20082706

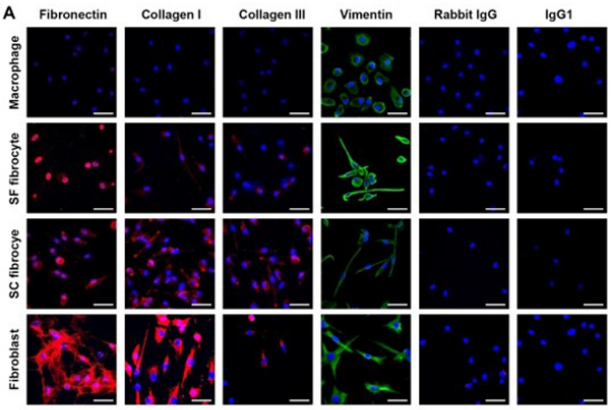

Immunofluorescence Microscopy
Fibrocytes were generated from PBMC under serum-free (SF) and serum-containing (SC) culture conditions, as well as macrophages. Fibroblast cell lines were included as a positive control for stromal cell markers. Immunostaining is shown in red for the stromal markers fibronectin, collagens I and III and their rabbit IgG control, with vimentin and its mouse IgG1 control in green (A). Nuclear staining is shown in blue. Bar represents 50 µm. Data are representative of at least two separate experiments. Fig 2. PMID: 20305780

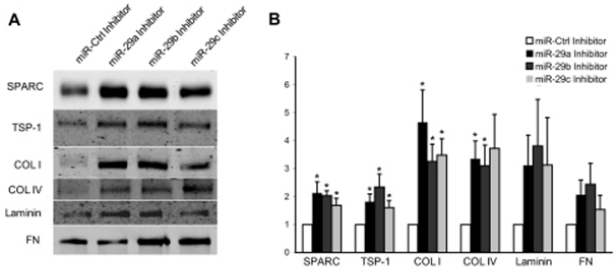

Western Blot
Inhibition of the miR-29 family induces ECM synthesis. (A) Representative immunoblot and (B) densitometric analyses of ECM proteins from conditioned media of TM cells transfected with miR control, miR-29a, miR-29b, or miR-29c inhibitors. All data are expressed as the mean ± SEM (*P < 0.05 vs. corresponding miR-Ctrl Inhibitor group; n = 5, where n refers to the number of independent experiments performed using n different primary human TM cell strains). Fig 5. PMID: 21330653

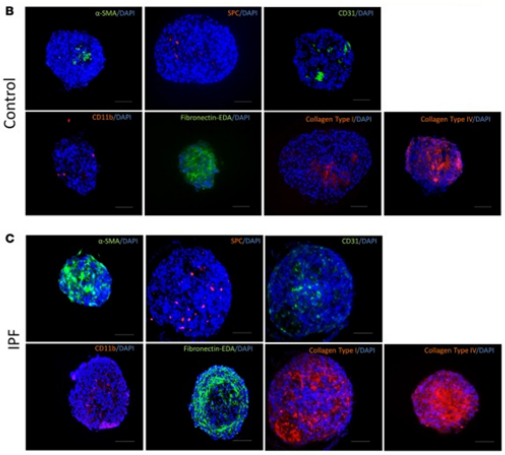

Immunofluorescence Microscopy
(B) Immunofluorescent staining of pulmospheres from IPF patients for α-SMA, SPC, CD31, CD11b, fibronectin-EDA, collagen type I, and collagen type IV in paraffin-embedded sections. All immunofluorescent slides were costained with DAPI for nuclei. Five random pulmospheres were sampled from each control subject (n = 9). Scale bar: 250 µm. (C) Immunofluorescent staining of pulmospheres from IPF patients for α-SMA, SPC, CD31, CD11b, fibronectin-EDA, collagen type I, and collagen type IV in paraffin-embedded sections. All immunofluorescent slides were costained with DAPI for nuclei. Five random pulmospheres were sampled from each IPF patient (n = 20). Scale bar: 250 µm. Fig 1. PMID: 28138565

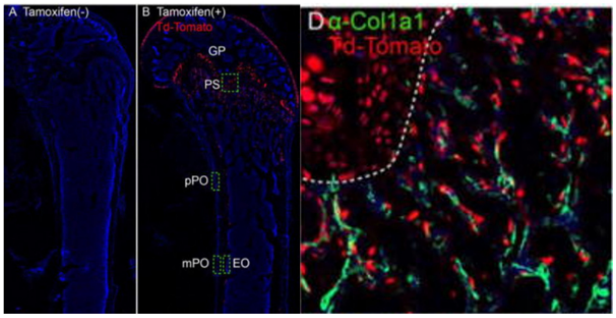

Immunofluorescence Microscopy
Short term Sox9CreErt2:Td-Tomato lineage tracing in representative frozen sections of intact adult mouse femora. The contribution of Td-Tomato positive cells was examined in the femurs of uninjected control (A) and TM-injected mice (B) 14 days after a final TM injection. In the primary spongiosa/growth plate area, expression and cellular localization of Col1a1+ osteoblasts (D). Fig 1. PMID: 28627474

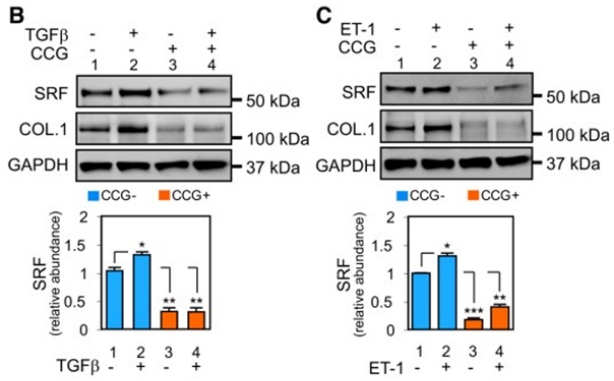

Western Blot
B and C: rat HSCs were cultured as in methods and then exposed to transforming growth factor-β (TGF-β; 10 ng) or endothelin-1 (ET-1; 20 nM) for 24 h. SRF and COL.1 expression was measured as in A. Results are presented as in A (n = 3 repeats/group, *P < 0.05, **P < 0.01, ***P < 0.001). Fig 5. PMID: 31928221

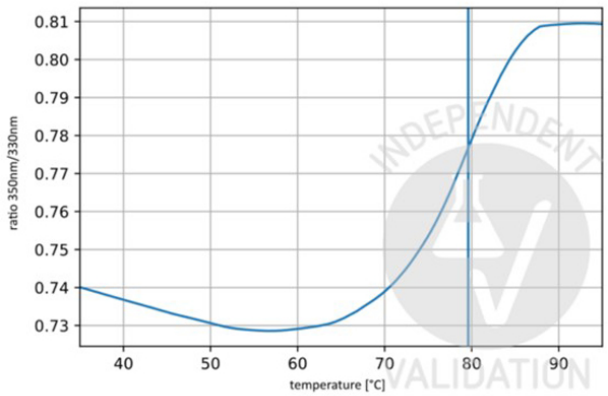

Figure
Unfolding profile of Rabbit Anti-Collagen Type I.
The fluorescence signal is plotted against temperature. The vertical line indicates the Ti at 79.6 °C. Independently Validated by antibodies-online GmbH (p/n ABIN7565871/ ABIN5596819/ ABIN5596820) courtesy of NanoTemper Technologies.

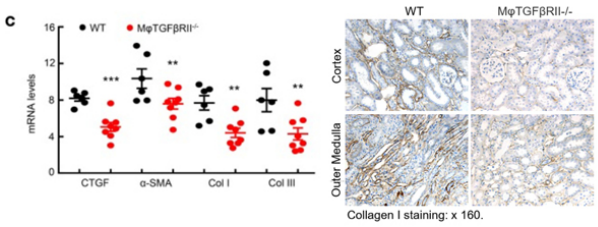

Immunohistochemistry
(C) Macrophage TGF-βRII deletion led to decreases in mRNA levels of profibrotic and fibrotic CTGF, collagens I and III (Col I and Col III), and α-SMA. **P < 0.01, ***P < 0.001. n = 6 in Tgfbr2fl/fl (WT) mice, and n = 8 in macrophage TGF-βRII–/– mice. Fig 2. See additional IHC SF8.
PMID: 30385721

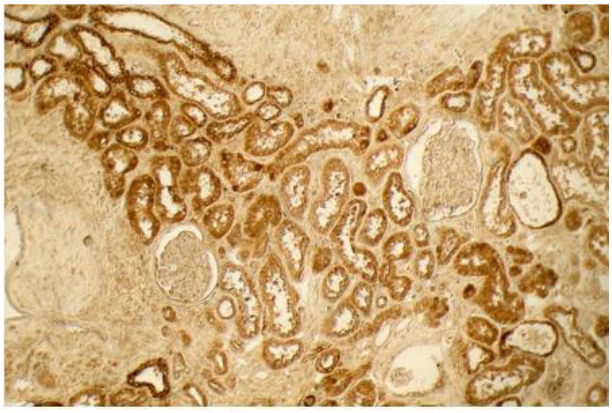

Immunohistochemistry
Rockland's Affinity Purified anti-Collagen I antibody was used at a 1:100 dilution to detect distal tubules in normal kidney tissue. Note the absence of staining of glomeruli. The antibody was reacted with antibody for 4 hours at room temperature followed by the addition of secondary antibody and substrate reaction. Tissue was formalin-fixed and paraffin embedded. No antigen retrieval was performed.

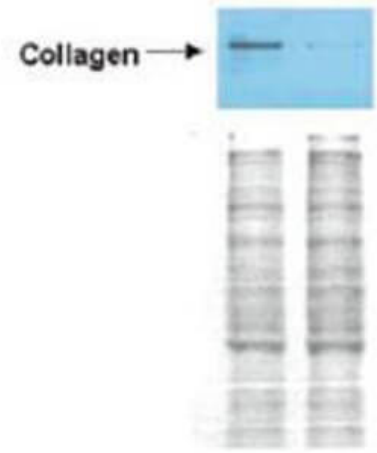

Western Blot
Western blot analysis is shown using Rockland's Affinity Purified anti-Collagen I antibody to detect expression of collagen I in Wistar rat hepatic stellate cells (HSC) in control (GFP-transduced) (left lane) and PPARg-transduced cell lysates (right lane). Protein staining shown below each blot depicts equal protein loading. An equal amount of the whole cell protein (100 µg) was separated by SDS-PAGE and electroblotted to nitro-cellulose membranes. Proteins were detected by incubating the membrane with anti-Collagen I antibody at a concentration of 0.2–2 µg/10 ml in TBS (100 mM Tris-HCl, 0.15 M NaCl, pH 7.4) with 5% Non-fat milk. Detection occurred by incubation with a horseradish peroxidase-conjugated secondary antibody at 1 µg/10 ml. Proteins were detected by a chemiluminescent method using the PIERCE ECL kit (Amersham Biosciences). Other detection systems will yield similar results. See Hazra et al. (2004) for additional details.

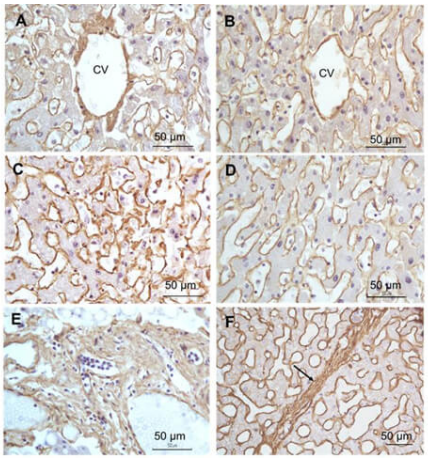

Immunohistochemistry
Immunohistochemistry of Rabbit Anti-collagen type I antibody. Tissue: right lobe of the liver section. A:Central Vein (CV) fibrosis, B: Non-fibrotic CV, C: Perisinusodial fibrosis, D: Non-fibrotic area, E: Protat tract fibrosis, F: Septal fibrosis (arrow). Fixation: formalin fixed paraffin embedded. Antigen retrieval: not required. Primary antibody: Anti-collagen type I at 1:1250 for 4°C for 24hr. Secondary antibody: Peroxidase biotin-streptavidin rabbit secondary antibody at 1:10,000 for 45 min at RT. Localization: Anti-collagen type I is intra and extracellular. Staining: 3.3'-diaminobenzidine tetrahydrochloride was used as the chromogen. Nuclei were counterstained purple with hematoxylin.

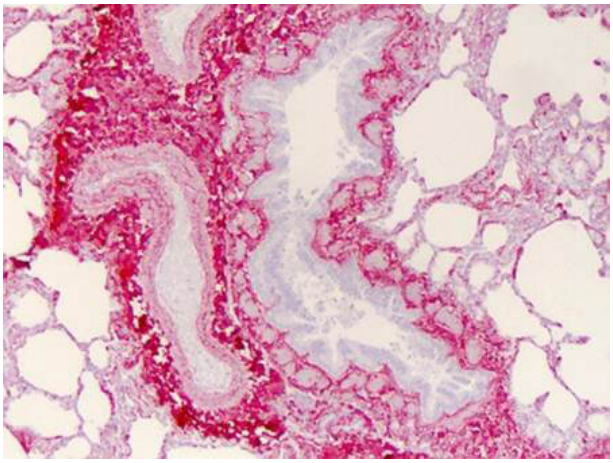

Immunohistochemistry
Immunohistochemistry of Collagen I antibody. Tissue: human lung. Fixation: formalin fixed paraffin embedded. Antigen retrieval: user optimized. Primary antibody: Collagen 1 1:400 Secondary antibody: Peroxidase goat anti-rabbit at 1:10,000 for 45 min at RT. Localization: Strong staining was observed in the extracellular matrix of the lung. Epithelial cells were negative. Staining: antibody as precipitated red signal with a hematoxylin purple nuclear counterstain.

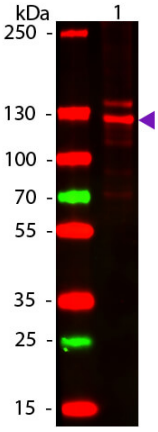

Western Blot

Western blot of Human Collagen Type I. Lane 1: Human Collagen Type 1 (p/n 009-001-103). Load: 50 ng per lane. Primary antibody: Collagen Type I antibody at 1:1,000 overnight at 4°C. Secondary antibody: DyLight™ 649 rabbit secondary antibody (p/n 611-743-127) at 1:20,000 for 30 min at RT. Block: (p/n MB-070(for 30 min at RT. Predicted/Observed size: 139 & 130 kDa, 139 & 130 kDa for Collagen Type I. Other Band(s): Collagen Type I splice variants and isoforms.

References

- Li, K et al. Scar-associated endothelial-stellate cellular crosstalk drives fibrosis resolution in MASH. *Cell Reports* (2026)
- Queiroz ZAJ et al. Type V Collagen as a Critical Regulator of Fibrillar Matrix Remodeling in a Murine Model of Systemic Sclerosis. *Cells.* (2025)
- Liu M et al. Effects of Brimonidine, Latanoprost, and Omidenepag on Tunicamycin-Induced Endoplasmic Reticulum Stress and Fibrosis in Human Trabecular Meshwork Cells. *Biomolecules.* (2025)
- Chang J et al. Endocytic recycling is central to circadian collagen fibrillogenesis and disrupted in fibrosis. *Elife.* (2025)
- Ito S et al. Heterozygous Tcf4 Deficiency Mitigates Fuchs Endothelial Corneal Dystrophy Progression in a Mouse Model. *Invest Opthalmol Vis Sci.* (2025)
- Silveira MJ et al. Immunostimulatory effects of IL-12 targeted pH-responsive nanoparticles in macrophage-enriched 3D immuno-spheroids in vitro model. *Drug Deliv Transl Res.* (2025)
- Brownell D et al. Impact of the Use of 2-Phospho-L Ascorbic Acid in the Production of Engineered Stromal Tissue for Regenerative Medicine. *Cells.* (2025)
- Omori-Miyake M Loss of Bach2 in T cells causes prolonged allergic inflammation through accumulation of effector T cells and disruption of epidermal barrier. *J Allergy Clin Immunol.* (2025)
- Baldavira CM et al. Matrisome analysis of NSCLC unveils clinically-important cancer-associated extracellular matrix changes. *Biochim Biophys Acta Mol Basis Dis.* (2025)
- Elia A et al. Amyloid β instigates cardiac neurotrophic signaling impairment, driving Alzheimer's associated heart disease. *bioRxiv [preprint]* (2025)
- Poret JM et a. Chronic binge alcohol dysregulates omental adipose tissue extracellular matrix in simian immunodeficiency virus-infected macaques. *Alcohol Clin Exp Res (Hoboken).* (2025)
- da Silva AF et al. Cigarette Smoke Exposure Leads to Organic and Mineral Bone Component Changes: The Importance of Rho Kinase Function in These Events. *Cells.* (2025)
- Tanaka T et al. Clinicopathological findings in refractory diabetic macular edema: A case report. *Biomed Rep.* (2024)
- Silva ED et al. Pericardial Fluid Accumulates microRNAs That Regulate Heart Fibrosis after Myocardial Infarction. *Int J Mol Sci.* (2024)
- Fernandes S et al. TGF-β induces matrisome pathological alterations and EMT in patient-derived prostate cancer tumoroids. *Matrix Biol.* (2024)
- Podolsky MJ et al. Genome-wide screens identify SEL1L as an intracellular rheostat controlling collagen turnover. *Nat Commun.* (2024)
- View More ...

Disclaimer

This product is for research use only and is not intended for therapeutic or diagnostic applications. Please contact a technical service representative for more information. All products of animal origin manufactured by Rockland Immunochemicals are derived from starting materials of North American origin. Collection was performed in United States Department of Agriculture (USDA) inspected facilities and all materials have been inspected and certified to be free of disease and suitable for exportation. All properties listed are typical characteristics and are not specifications. All suggestions and data are offered in good faith but without guarantee as conditions and methods of use of our products are beyond our control. All claims must be made within 30 days following the date of delivery. The prospective user must determine the suitability of our materials before adopting them on a commercial scale. Suggested uses of our products are not recommendations to use our products in violation of any patent or as a license under any patent of Rockland Immunochemicals, Inc. If you require a commercial license to use this material and do not have one, then return this material, unopened to: Rockland Inc., P.O. BOX 5199, Limerick, Pennsylvania, USA.